Phthalonaphthalocyanines: New Far-Red Dyes for Spectral Hole Burning

Indrek Renge,*,† Heinz Wolleb,‡ Heinz Spahni,‡ and Urs P. Wild

Physical Chemistry Laboratory, ETH-Zentrum, CH-8092 Zürich, Switzerland, and Ciba Research Center Marly, CH-1723 Marly 1, Switzerland

Received: May 14, 1997[⊗]

Mixed phthalocyanines carrying one anthracene (Pc_3An) or substituted naphthalene nucleus (Pc_3NcR_2, R = H, OCH_3, or $SC_{12}H_{25}$) are proposed as low-temperature photochroms for spectral hole burning. Solubility of these compounds in polymers was greatly enhanced by introducing the 2,4-dimethyl-3-pentoxy substituent to the remaining three benzopyrrolic fragments. The wavelengths and intensities of the Q transitions (S_1 and S_2) were measured for two prototropic tautomers having different position of the pair of inner protons. The average energy of the two lowest transitions is very similar in both tautomers, although the S_1-S_2 splitting is much smaller in the less stable form. The relative equilibrium concentration of the tautomers at room temperature depends on the electron releasing properties of the substituents. This allows one to predict the positions of protons in each form. Absorption dichroism of stretched polyethylene films was used in order to establish the direction of the S_1 and S_2 transition dipole moments in the molecular framework. The tautomers can be completely converted into each other at 10 K by light with quantum yields of $(1-2) \times 10^{-3}$ and $(5-8) \times 10^{-3}$, respectively, depending on the direction of the process. Most probably the phototransformation occurs in the vibrationally relaxed triplet state via the tunneling of a single proton which results in an intermediate state with *cis*-configuration of protons. The photochemically accumulated less stable form decays at higher temperatures (T) as a result of a thermally activated tunneling process at characteristic T of 115 and 153 K for protonated and deuterated Pc_3Nc, respectively. The strength of linear electron−photon coupling (EPC), which is crucial from the point of view of spectral hole burning, is characterized by Debye−Waller factors (DWFs) about 0.6−0.75, depending on the compound and the polymer matrix. The T dependence of quasihomogeneous hole width (Γ_{qh}) obeys a power law with coefficients 2.5 ± 0.5 (between 6 and 30−45 K). In different polymer hosts, the DWF increases and the hole width decreases in the following order: polystyrene > poly(vinyl butyral) > polyethylene. The strength of EPC for the lowest transitions is similar in both tautomeric forms. A slight enhancement of the EPC strength in the series of dyes $Pc_3Nc(OCH_3)_2 \sim Pc_3Nc < Pc_3Nc(SC_{12}H_{25})_2 < Pc_3An$ is correlated with the increase of electron-withdrawing power of substituents, plausibly, as a result of the increase of dipole moment change upon electronic excitation. Spectroscopic properties, phototautomerization quantum yields, and the EPC strength of mixed phthalocyanines were compared with those of chlorin and porphyrins.

Introduction

Spectrally very narrow persistent photobleaching of optical absorption (hole burning) was first demonstrated for frozen solutions of phthalocyanine in *n*-octane[1] and perylene and 9-aminoacridine in ethyl alcohol at 4 K.[2] Upon cooling, the former produces a snowy, microcrystalline solid, whereas the latter forms a transparent glass. Application of spectral hole burning for data storage, making narrow-band light filters, etc., obviously requires more convenient materials with better optical quality. We have found that it is possible to polymerize styrene without initiators in sealed ampoules at 120−160 °C without destroying the octaethylporphine additive.[3] Pressing the obtained cylindrical polymer pieces between flat glass surfaces at 150−170 °C yielded 1−5 mm thick plates with sufficiently good optical quality for recording frequency- and time-domain holograms.[4] Another method, casting of optically clear polymer films from solutions was utilised for preparation of thin (0.05−0.5 mm) chlorin-doped poly(vinyl butyral) samples which enabled one to realize holographic detection of small holes.[5,6] Recently, the possibility to store 10^4 holograms in the 12 nm spectral range has been demonstrated in the same material.[7] The alkyl-substituted porphine derivatives possess the smallest electron−phonon coupling strength among the organic dyes and pigments,[8] allowing one to create the most deep and narrow spectral holes. The virtues of chlorin (dihydroporphine) are the much larger absorption cross-section than that of the porphyrins, and more importantly, the spectral blue shift of the photoproduct from the actual burning region.[9,10] As a result, spectral holes can be burned over the whole inhomogeneous S_1 band, with minimum interference with the previously recorded images. Unfortunately, the quantum yield of the photobleaching in chlorins is by 2 orders of magnitude smaller than that in porphyrins.

The aim of the present work was the preparation of chromophores which absorb light in the output region of the Ti:sapphire laser (750−780 nm) and possess the hole-burning properties not worse than porphyrins and chlorins. For the first time, considerable synthetic efforts were undertaken in order to achieve the spectral separation of the educt and the product bands as well as the good solubility of the pigment in liquids and polymers. Two molecular axes passing the pyrrolic nitrogens in tetrapyrrolic macrocycle were rendered inequivalent by replacing one of the benzo fragments in phthalocyanine by

† Permanent address: Institute of Physics, EE2400 Tartu, Estonia.
‡ Ciba Research Center Marly.
⊗ Abstract published in *Advance ACS Abstracts,* August 1, 1997.

S1089-5639(97)01586-7 CCC: $14.00 © 1997 American Chemical Society

naphthalene or anthracene nuclei. Bulky 2,4-dimethyl-3-pentoxy substituents were introduced to the benzo rings with the goal to increase greatly the solubility, so that 0.01 mm films with optical density about unity could be easily prepared. The first results of optical experiments with polymer films containing phthalonaphthalocyanines have been already reported in ref 11.

The properties of mixed phthalonaphthalo- (Pc_3Nc) and -anthracenocyanines (Pc_3An), which are essential for high-density optical storage, are characterized in this study. In the first section the general spectroscopic and structural features are described, such as the assignments, intensities, and solvent shifts of the visible absorption bands, the directions of transition dipoles, and the positions of central protons in each tautomeric form. The second part deals with the quantum efficiency of tautomerization and the mechanism of photoinduced and thermal proton migration. The characteristics of electron−phonon coupling processes, such as the shape of the phonon wing, the Debye−Waller factor and the temperature dependence of quasihomogeneous hole width, which are of particular importance in spectral hole burning, are discussed in the last section.

Experimental Section

1. Synthesis of Starting Materials. *3-(2,4-Dimethyl-3-pentoxy)phthalonitrile* (**1**). In a 1.5 L three-necked round-bottomed flask, equipped with a stirrer and a thermometer, were charged 141.1 g (0.815 mol) of 3-nitrophthalonitrile, 104.1 g (0.897 mol) of 2,4-dimethyl-3-pentanol in 815 mL of *N*,*N*-dimethylformamide (DMF). The resulting solution was cooled to −10 °C under argon and then 39.1 g (0.897 mol) of NaH was added in portions within 2 h. The resulting solution was stirred at −15 °C for 3 h and then added drop by drop to 4 L of water. The resulting suspension was filtered, and the residue was washed three times with 1 L of water and dried at 60 °C/125 Torr overnight. The product was crystallized from 3.8 L of hexane. Yield: 154.9 g (78.5%), mp 83.0−83.5 °C. TLC (hexane/ethyl acetate 8:1): $R_f = 0.75$.

6,7-Dimethoxy-naphthalene-2,3-dicarbonitrile (**2**). This compound was prepared starting from 4,5-dimethoxybenzene-1,2-carbonitrile[12] and succinonitrile in DMSO/K_2CO_3 (DMSO = dimethylsulfoxide).[13]

Anthracene-2,3-dicarbonitrile (**3**). In a 100 mL round-bottomed flask, equipped with a reflux condenser and a stirrer, were charged 25.4 g (95.4 mmol) of anthracene-2,3-dicarboxylic acid[14] and 34 g of acetic anhydride. The suspension was heated with reflux for 3 h, cooled to 0 °C, and filtered. The residue was washed with 100 mL of cold *n*-pentane and dried at 50 °C/125 Torr overnight. Yield of anhydride: 21.1 g (89%) as a brown solid.

This product was charged in a 250 mL round-bottomed flask, equipped with a reflux condenser and a stirrer, together with 11.43 g (0.25 mol) of formamide and 100 mL of xylene. The resulting suspension was heated with reflux for 24 h, cooled to room temperature and filtered, and the residue was washed with 100 mL of *n*-pentane. The brown raw material was recrystallized from 250 mL of DMF. Yield of imide: 20.8 g (99.4%) as off white crystals. Anal. Calcd for $C_{16}H_9NO_2$: C 77.72, H 3.67, N 5.67. Found: C 76.90, H 3.79, N 5.36.

This product was reacted in an autoclave together with 100 mL of 25% NH_3 in water: at 80 °C for 24 h. The resulting yellow suspension was evaporated. Yield of diamide: 23.0 g (102.4%) as off white solid. Anal. Calcd for $C_{16}H_{12}N_2O_2$: C 72.72, H 4.58, N 10.60. Found: C 72.88, H 4.26, N 8.90%.

In a 250 mL three-necked round-bottomed flask, equipped with a stirrer, were charged 13.0 g (48.2 mmol) of the diamide and 140 mL of pyridine. The resulting yellow suspension was cooled to 3 °C under argon and then 18.8 g (0.12 mol) of $POCl_3$ were added drop by drop within 30 min. The resulting brown suspension was warmed to room temperature and stirred for 1.5 h. The reaction mixture was poured in 1 L of water, and the resulting suspension was filtered. The residue was washed with 500 mL of water and dried at 70 °C/125 Torr overnight. The resulting crude material (12.2 g) was purified by flash chromatography on 220 g of silica gel with hexane/ethyl acetate 1:1 as eluent. Yield: 1.05 g (9.4%) of a yellow powder. TLC (hexane/ethyl acetate 5:1): $R_f = 0.69$. Anal. Calcd for $C_{16}H_8N_2$: C 84.19, H 3.53, N 12.27. Found: C 81.65, H 3.76, N 10.37. Attempts to further purify this product failed.

2. Synthesis of Unsymmetrical Phthalonaphthalocyanines. *Pc_3Nc* (**4**). In a 3.5 L three-necked round-bottomed flask, equipped with a stirrer, a reflux condenser, and a thermometer, were charged 1.8 L of methoxyethanol and heated under nitrogen to 50 °C. Lithium powder [19.2 g (2.7 mol)] was added in small portions with 4 h keeping the temperature at 50 °C. **1** [60.5 g (0.25 mol)] and 4.9 g (0.0275 mol) of naphthalene-2,3-dicarbonitrile were added, and the resulting solution was heated with reflux for 18 h. The resulting green solution was cooled to room temperature, 1 L of acetic acid was added drop by drop within 1 h, and the solution was stirred for 30 min. The solution was evaporated, the residue was dissolved in CH_2Cl_2, 100 g of silica gel was added, and the slurry was evaporated. The green powder was placed on top of a column with 500 g of silica gel, and the symmetrical side product ($R_f = 0.73$) and the product ($R_f = 0.57$) were eluted with hexane/ethyl acetate 10:1. The fractions containing the desired product were collected, evaporated, and subjected to a second chromatography. Yield: 1.05 g (4.2%) of **4** as a green powder. TLC (hexane/ethyl acetate 10:1): $R_f = 0.57$. UV (NMP): $\lambda_{max} = 757/715$ nm. PD-MS (PD-MS = plasma desorption mass spectrometry): $(M + H)^+ = 907.5$.

$Pc_3Nc(OCH_3)_2$ (**5**). In the same manner, 9.2 g (38.15 mmol) of **1** and 1 g (4.19 mmol) of **2** were reacted. The crude product was purified twice with column chromatography (hexane/ethyl acetate = 7.3) to yield 0.15 g (1.5%) **5** as a green powder. TLC (hexane/ethyl acetate 7:3): $R_f = 0.69$. UV (NMP): $\lambda_{max} = 757/718$ nm. PD-MS: $(M + H)^+ = 969.9$.

$Pc_3Nc(SC_{12}H_{25})_2$ (**6**). In the same manner, 21.2 g (87.50 mmol) of **1** and 5.62 g (9.71 mmol) of 6,7-dodecylthionaphthalene-2,3-dicarbonitrile[15] were reacted. The crude product was purified twice with column chromatography (hexane/ethyl acetate 7:1) to yield 0.61 g (4.8%) of **6** as a green powder. TLC (hexane/ethyl acetate 7:1): $R_f = 0.75$. UV (NMP): $\lambda_{max} = 760/724$ nm. PD-MS: $(M + H)^+ = 1309.1$.

Pc_3An (**7**). In the same manner, 9.55 g (39.43 mmol) of **1** and 1 g (4.38 mmol) of **3** were reacted. The crude product was purified with column chromatography (hexane/ethyl acetate 7:3). The fractions containing the desired product were evaporated, and the residue was dissolved in 15 mL toluene and added drop by drop to 300 mL of methanol. The precipitated product was isolated by filtration and dried at 60 °C/125 Torr overnight to yield 0.15 g (1.5%) **7** as a green powder. TLC (hexane/ethyl acetate 9:1): $R_f = 0.49$. UV (NMP): $\lambda_{max} = 783/735/708$ nm. MALDI-MS (MALDI-MS = matrix-assisted laser desorption/ionization mass spectrometry): $(M + H)^+ = 958.8$.

The chemical structure of the more stable tautomer (see below) of mixed Pc_3Nc's (**4**−**7**) is shown in Figure 1.

3. Other Dyes and Sample Preparation. Pure sample of chlorin was prepared by G. Grassi at ETH. The remaining pigments were purchased from Aldrich and used as received.

The acrylic and olefinic photopolymers doped with phtha-

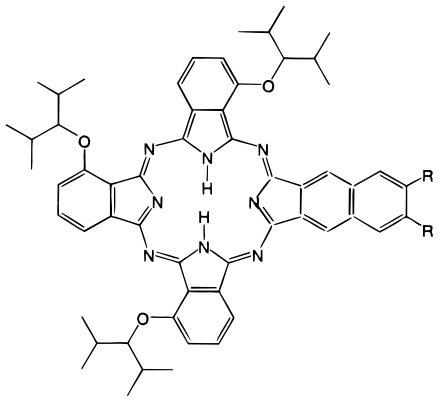

4 R=H
5 R=OCH_3
6 R=$S(CH_2)_{11}CH_3$
7 2R=

Figure 1. Chemical structure of phthalonaphthalo/anthracenocyanines Pc_3NcR_2 and Pc_3An. The configuration of protons in the stable tautomer is shown.

locyanines were produced in Marly by N. Bogdanova-Arn and A. Mühlebach, respectively. Polyethylene (PE), polystyrene (PS, average M_w 280 000) and poly(vinyl butyral-*co*-vinyl alcohol-*co*-vinyl acetate) (88% PVB, M_w 50 000−80 000) were from Aldrich. PVB and PS were dissolved in CH_2Cl_2 and PE in hot toluene, and a small amount of dye was added. The solution was cast on a Petri dish and left slightly covered for drying (occasionally on a warm hot plate). The residual solvent was removed with heating at 100 °C in vacuum during a period of several days. The transparency of PE can be improved by pressing a piece of material between the glass slides on a hot plate, followed by fast quenching in liquid N_2. The films were 0.05−0.2 mm thick and had the optical density at the absorption maximum of 0.7−1.3

4. Spectral Measurements. Absorption spectra were recorded on a Perkin-Elmer Lambda 9 spectrophotometer. For measurements at low temperatures, it was equipped with model CF1204 continuous flow cryostat connected to the ITC-4 temperature controller (both Oxford).

Holes were burned with a Lambda Physik dye laser LPD 3002E (line width 2.5 GHz, pulse length ∼10 ns) pumped with an excimer laser LPX 100. Low energy density and high pulse frequency (100 Hz) were utilized in order to minimize the population of the triplet state. For determination of hole-burning quantum yields and Debye−Waller factors, the film was irradiated directly in the sample compartment of spectrophotometer. In order to avoid possible shifts of the base line upon turning the sample, the film was fixed at an angle of 45° relative to both the laser beam and the probe beam. The laser beam was rendered circularly polarized to avoid the photoselection effect, as the probe beam of the spectrophotometer is predominately horizontally polarized. The hole was burned by scanning the laser over 0.2 nm. The spectra were recorded over the broad range (10 nm) with the same slit width. The 0.2 nm slit width ensures both an acceptable signal-to-noise ratio and the separation of the zero-phonon line from the wings. Debye−Waller factor was determined as a square root of the integrated intensity ratio of the small (less than 10% of limiting depth) zero-phonon hole to the total loss of absorption intensity.

Quasihomogeneous width was determined for shallow holes (less than 5−7% of the optical density change). Holes were explored in transmission by scanning the dye laser with

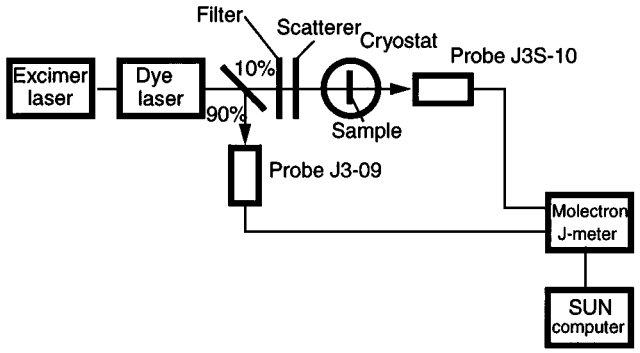

Figure 2. Setup for detection of spectral holes in transmission by means of a tunable pulsed dye laser. The pulse-to-pulse instability of the excimer/dye laser is reduced by two-channel detection. The monitoring light is divided by a beam splitter in such a way that 90% of the intensity is incident on a less sensitive detector J3-09.

attenuated energy. In this case, detection was accomplished in a two-channel setup using a Molectron JD2000 joulemeter ratiometer with a sensitive J3S-10 (1 kV/μJ) probe in the sample channel and a less sensitive one, J3-09 (1 V/mJ) as a reference (Figure 2). Laser was operated with the frequency of 40 Hz. Signals of the two channels were divided, averaged (over 10 Hz) and fed into the SUN computer. Typically, 400 data points/scanning interval were collected. The signal-to-noise ratio of 0.5% was reached after removing the interference beats by placing a scattering piece of tape on the cryostat window. The transmission signal was converted to logarithmic units and fitted with a Lorentzian function. The instrumental contribution of 5 ± 0.5 GHz was subtracted from the measured hole width.

Results and Discussion

1. Spectroscopy and Structure of Tautomeric Forms. *1.1. Transition Energies and Intensities*. Absorption spectra of Pc_3Nc, $Pc_3Nc(OCH_3)_2$ and Pc_3An in the region of Q transitions in low-density polyethylene (PEld) at 10 K are displayed in Figure 3a−c. Extensive transformation of the spectrum occurs under illumination with white light. Photoequilibrium is reached already in less than 100 s at the intensities of 100 mW/cm^2. Larger amounts of the photoproduct can be accumulated upon the laser irradiation to the first (S_1) (Figure 3a) or second absorption band of the educt (S_2) (Figure 3c). Warming the system up to 200 K restores the spectrum of the sample frozen in the dark. The presence of isosbestic points indicates that two mutually interconvertible species are present. These two forms can be assigned to the prototropic tautomers with different positions of proton pairs at pyrrolic nitrogen atoms. We designate these forms as the stable (e.g., Pc_3Nc) and less stable tautomer (e.g., Pc_3Nc*), or educt and product, respectively. It is reasonable to assume that the visible spectrum of phthalocyanines consists only of two purely electronic transitions (S_1 and S_2) accompanied by their vibronic replicas (S_{11}, S_{21}, etc.).[16,17] The transitions in the product are marked by a star (S_1*, S_2*, etc.).

The assignment of the observed broad bands was carried out by using spectral hole burning, dichroism of stretched films, as well as solvent and temperature induced shifts of the band maxima. Photobleaching of the S_1 band and its vibrational satellite S_{11} with the laser light results in narrow spectral holes. The S_2 transition usually yields broad holes as a result of ultrafast relaxation (<1 ps) to the S_1 state.

The absorption peak positions of (na)phthalocyanines and several reference compounds in PEld at 10 K are collected in Table 1. The spectra of stable tautomers are very similar to those of parent phthalocyanine (Pc) and its symmetrically

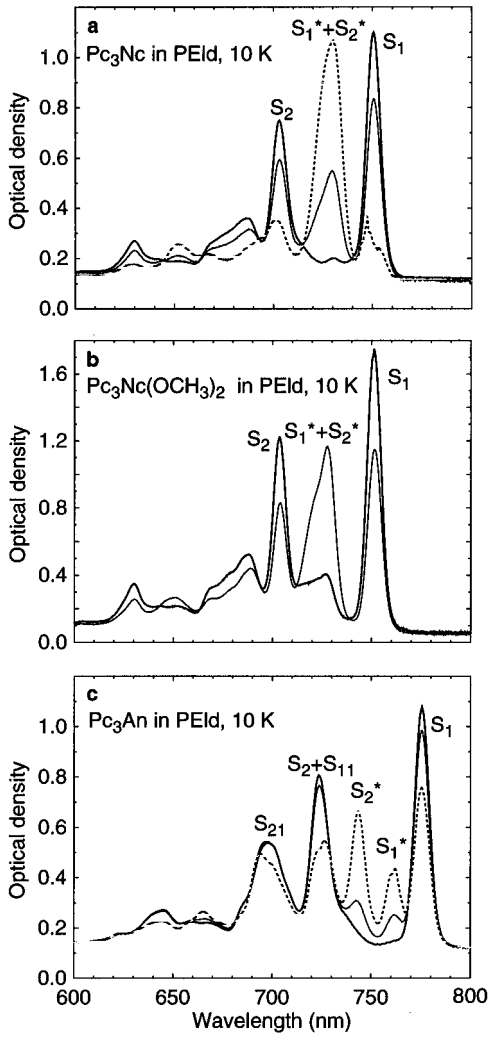

Figure 3. Absorption spectra of phthalonaphthalo/anthracenocyanines in low-density polyethylene films at 10 K frozen in the dark (thick solid line) and after irradiation with white light (100 s, 100 mW/cm^2) (thin solid line). Additional amount of less stable tautomer was accumulated by scanning the laser over the S_1 band of Pc_3Nc between 745 and 760 nm (3 J/cm^2) (a) or over the S_2 band of Pc_3An between 720 and 725 nm (0.4 J/cm^2) (c) (dotted line).

substituted derivatives. A comparison of spectral maxima of symmetrical *t*-Bu−Pc, Pc{OCH[CH(CH$_3$)$_2$]} and the unsymmetrical compounds reveals that both the alkoxy substitution and an extra naphthalene or anthracene fragments contribute to the bathochromic shifts of Q bands in Pc_3Nc's and Pc_3An.

It follows from the molecular symmetry considerations that directions of the Q transition dipoles should be oriented along the mutually perpendicular pyrrolic N···N and N−H···H−N axes of the macrocycle. Therefore, the S_1-S_2 splitting in tetrapyrrolic pigments reflects the degree of inequivalence of the two perpendicular axes passing through the pyrrolic rings. In free-base derivatives with four identical pyrrolic fragments, the S_1-S_2 distance decreases fast with the increasing size of molecules (e.g., *t*-Bu TAP (2032 cm^{-1}) > *t*-Bu−Pc (848 cm^{-1}) > *t*-Bu−Nc (243 cm^{-1})), because the large π-electronic system is less influenced by the position of protons in the center of macrocycle. The Q transitions become degenerate in metal complexes of tetrapyrrolic ligands with D_{4h} symmetry.[16]

Spectra of less stable tautomeric forms show smaller S_1*−S_2* distances than the main forms. In Pc_3An* the S_1* and S_2* band separation is 312 cm^{-1}, whereas in the stable tautomer the S_1-S_2 interval is 924 cm^{-1}. In Pc_3Nc* and $Pc_3Nc(OCH_3)_2$* the S_2* band appears as a shoulder, so the S_2*−S_1* splitting should be less than 200 cm^{-1}. Remarkably, average energy of the Q transitions ($^1/_2(S_1 + S_2)$ and $^1/_2(S_1* + S_2*)$) remains very close for both tautomeric forms. Similar rules apply for chlorin, despite the very large differences in the spectra of educt and product. It is probable that the S_1*−S_2* splitting in chlorin (photo)product is small (∼150 cm^{-1}),[10] and thus the average Q band energies of both forms are similar (Table 1). Moreover, the mean Q band energies are approximately constant in the tautomers of asymmetrically substituted porphyrins as well.[18,24] In contrast to Pc's and chlorins, the S_1* band of less stable tautomers of the porphyrins is bathochromically shifted.[18,24,25]

On the other hand, the frequency difference between the respective transitions in prototropic tautomers or the S_1-S_1* or S_2-S_2* distances should originate from the inequivalence of N−N axes of the tetrapyrrolic ligand without protons (dianion). Similarly, the S_1-S_2 energy splitting in the metal complexes depends also on the deviations of the macrocyclic ligand from the D_{4h} symmetry point group. It follows from Table 1 that the tautomeric shift S_1-S_1* in free-base molecule and the S_1-S_2 splitting in its Mg or Zn complex are of comparable magnitude: for Pc_3Nc 379 and 391, protopheophytin/protochlorophyll −337[18] and 350−500,[19] chlorin ∼1600[9,10] and 1000−2000,[21,22] and pheophytin/chlorophyll *a* ∼500[23] and 750−900 cm^{-1},[19] respectively.

As far as the two Q transition dipoles pass the opposite pyrrolic nitrogen atoms and are mutually perpendicular, the magnitude of S_1-S_2 splitting in tetrapyrrolic macrocycles can be regarded as a measure of the equivalence of these two axes. This inequivalence is determined by two factors: the presence of a pair of central protons and the differences in pyrrolic rings. The influence of these factors can be treated as additive. Thus the greatly reduced Q level splitting in less stable tautomers in mixed (na)phthalocyanines and chlorins means that their π-electronic system has effectively a D_{4h} symmetry (i.e., the protons tend to compensate the influence of a modified pyrrole fragment).

The oscillator strength (*f*) of the S_1 bands of Pc_3Nc (peaking at 750.7 nm) and Pc_3An (775.3 nm) in toluene at 293 K was estimated according to the expression:[26]

$$f = (1/n)4.319 \times 10^{-9} \int \epsilon \, d\nu \qquad (1)$$

where *n* is the refractive index at the transition frequency (we use the value at sodium D line $n_D^{20} = 1.496$[27]) and ϵ is the extinction coefficient. The presence of an additional benzo ring slightly increases both the *f* and ϵ values from 0.124 ($\epsilon = (1.04 \pm 0.04) \times 10^5$ M^{-1} cm^{-1}) in Pc_3Nc to 0.143 ($(1.38 \pm 0.06) \times 10^5$ M^{-1} cm^{-1}) in Pc_3An.

Despite the rather drastic difference in the spectral shapes of tautomers, the integrated oscillator strength of the Q band region (550−800 nm) in Pc_3Nc and its OCH_3- and $SC_{12}H_{25}$-substituted derivatives diminishes only by 2.5 ± 0.3%. The Q bands of the Pc_3An* gain in intensity by 7% as compared to the educt absorption. In the case of chlorin, the visible absorption (450−600 nm) of the product is by 30% stronger than that of the educt (450−750 nm). The integration of spectra was carried out in the wavenumber scale (eq 1).

1.2. Absorption Spectra of Stretched Films. Pieces of doped low-density polyethylene (PEld) film were softened in a flow of warm air from a heat gun and stretched by hand during the cooling. The lengthening of the sample by a factor of 3−5 was achieved. Identical plastic polarizers were placed at the exit windows of the probe and reference light beams of the spectrophotometer. The sample film was affixed on the entrance window vertically relative to the stretching direction. Absorp-

TABLE 1: Q Band Absorption Maxima (cm^{-1}) of Tetrapyrrolic Pigments in Low-Density Polyethylene at 10 K[a]

	Q			Q*				
compound[b]	$\nu(S_1)$	$\nu(S_2)$	$\nu(S_2)-\nu(S_1)$	$\nu(S_1^*)$	$\nu(S_2^*)-\nu(S_1^*)$	$\nu(S_1^*)-\nu(S_1)$	$1/2[\nu(S_1)+\nu(S_2)]$	$^1/_2[\nu(S_1^*)+\nu(S_2^*)]$
			phthalonaphthalocyanines					
Pc_3Nc	13 325	14 226	901	13 704	<200	379	13 776	~13 800
c	13 251	14 128	877					
Zn−Pc_3Nc[d]	13 884	14 275	391					
$Pc_3Nc(OCH_3)_2$	13 311	14 213	902	13 744	<200	433	13 762	~13 800
$Pc_3Nc(SC_{12}H_{25})_2$	13 250	14 077	827	13 562		312	13 664	~13 650
Pc_3An	12 895	13 819	924	13 137	312	242	13 357	13 293
			symmetrical tetraazaporphyrins					
t-Bu−TAP	16 139	18 171	2032			~0		
Pc	14 446							
	15 132[e]	16 680[e]	1548[e]			0		
t-BuPc	14 336	15 184	848			~0		
Pc{OCH[$CH(CH_3)_2$]$_2$}[c]	13 647	14 286	639			~0		
t-Bu−Nc	12 762	13 005	243			~0		
			porphyrins and chlorins					
protopheophytin *a*[f]	15 674	17 762	2088	15 337	2978	−337	16 718	16 826
protochlorophyll			350, 500[g]					
chlorin	15 746[h]	19 410[h]	3664	17 416[i]	130−160?[i]	~1600[i]	17 578	~17 500
Zn−chlorin			103,[j] 2070,[k] 2350[l]					
pheophytin *a*						~500[m]		
chlorophyll *a*			750, 900[g]					

[a] Error ± 2 cm^{-1}; Q, stable tautomer; Q*, less stable tautomer (in case of free bases). [b] *t*-Bu, *tert*-butyl; TAP, tetraazaporphine; Pc, phthalocyanine; Nc, naphthalocyanine. [c] In olefinic photopolymer. [d] In *n*-heptane at 293 K. [e] In supersonic jet, ref 17. [f] A derivative of protochlorophyll in diethyl ether−tetrahydrofuran glass at 77 K, ref 18. [g] Reference 19. [h] In *n*-octane crystal at 4.2 K, ref 20. [i] In *n*-hexane crystal at 4.2 K, refs 9 and 10. [j] Reference 21. [k] For Zn−octaethylchlorin, ref 22. [l] For Zn−octaethylchlorin, ref 21. [m] Reference 23.

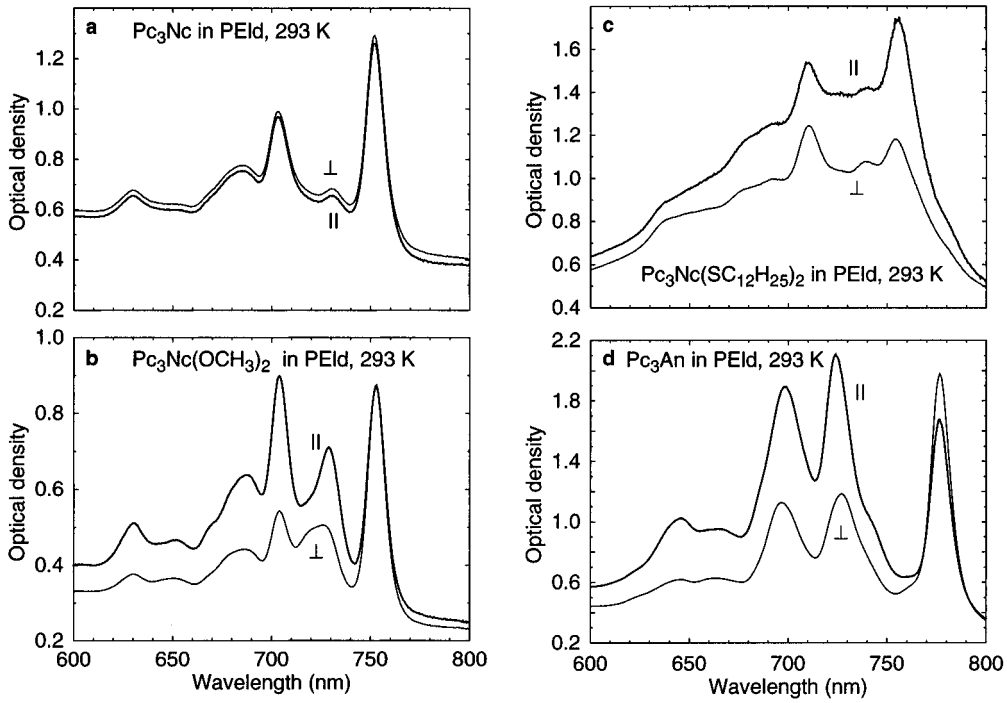

Figure 4. Absorption spectra of phthalonaphthalo/anthracenocyanines in stretched low-density polyethylene films at 293 K, recorded with the light polarization parallel (||) and perpendicular (⊥) with respect to the stretching direction.

tion spectra were recorded twice, with the polarizers oriented either vertically or horizontally (Figure 4).

In the case of unsubstituted Pc_3Nc, both absorption spectra are identical (Figure 4a). For (na)phthalocyanines carrying substituents at the naphthalene fragment, the relative intensity of S_1 and S_2 bands depends appreciably on the polarization direction of probing light. In $Pc_3Nc(OCH_3)_2$ and Pc_3An the S_2 band is much stronger than the S_1 band when the stretching direction and the polarization of light are parallel, whereas the opposite is true for $Pc_3Nc(SC_{12}H_{25})_2$ (Figure 4b−d). It is rather obvious that the substituted pigment molecules tend to align themselves along the axis passing the naphthalene fragment. Therefore, the S_1 transition dipole in $Pc_3Nc(SC_{12}H_{25})_2$ is parallel with the long axis. In both $Pc_3Nc(OCH_3)_2$ and Pc_3An the S_1 transition dipole passes through the identical benzopyrrolic rings. The sulphur containing dye is also somewhat different from the others by having slightly larger solvent shift of the S_1 band ($-p$ = 2400 cm^{-1}) than the remaining compounds ($-p$ = 2100−2200 cm^{-1}) (see below).

The shape of the 730 nm band in less stable tautomer $Pc_3Nc(OCH_3)_2$* undergoes noticeable changes depending on the polarization direction of light (Figure 2b), in particular at 10 K (not shown). This confirms that the broad band of less stable tautomer at 730 nm consists of two closely spaced transitions

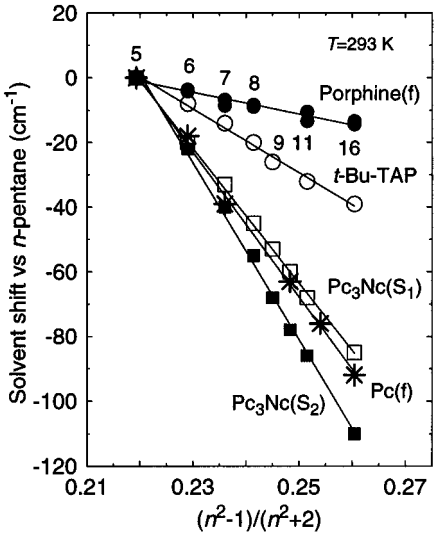

Figure 5. Solvent shifts of the absorption or fluorescence (f) band maxima in tetrapyrrolic chromophores in *n*-alkanes (relative to *n*-pentane) plotted vs Lorentz−Lorenz function of the solvent. Alkanes are denoted by their number of carbon atoms. The slope and intercept values of the linear plots (eq 2) are listed in Table 2.

with perpendicular dipole moments. Both the S_1* band of the product and the S_2 band of the educt show enhanced absorption for the parallel orientation of monitoring light. Consequently, in $Pc_3Nc(OCH_3)_2$, the S_1/S_1* transition dipole moment follows the direction of N−H···H−N axis (see section 1.4). The respective S_1/S_1* and S_2/S_2* transitions of both tautomers are mutually perpendicular.

1.3. Solvent Shifts of Absorption Bands. In the previous section, the optical transition energies were considered to be identical with absorption band maxima in polymer matrices. By contrast, the quantum chemical calculations would yield the energies of nonsolvated molecules. Therefore, it is necessary to determine to what extent the transition energies are changed by solvation. The 0-0 origins (ν_0^0) for bare cold molecules can be measured in supersonic expansions.[17,28] The ν_0^0 values may also be obtained by extrapolation of solvent shifts, recorded in liquid *n*-alkanes at room temperature, according to the expression (Figure 5):[29,30]

$$\nu = \nu_0 + p\phi(n^2) \qquad (2)$$

where ν is the band maximum, ν_0 and p are the regression parameters, and $\phi(n^2) = (n^2 - 1)/(n^2 + 2)$ is the Lorentz−Lorenz function of the refractive index for Na D line at 20 °C.

The intercept and slope values of eq 2 for mixed (na)-phthalocyanines and some simpler tetrapyrroles are listed in Table 2. The extrapolated vacuum frequencies ν_0 for porphine, chlorin, and phthalocyanine are red shifted relative to ν_0^0 in supersonic jets by 44, 55, and 110 cm^{-1}, respectively. Plausibly, the pure thermal effect owing to the electron-phonon coupling is responsible for this rather small shift.[31] It is absent, for example, in the low-temperature spectra of fullerenes in solid rare gases and frozen solvents.[31]

Because of different solvent shifts, the S_1-S_2 splitting in bare nonsolvated tetraazaporphines (including Pc and Pc_3Nc) is by 150−300 cm^{-1} (15−30%) larger than that in PEld (Tables 1 and 2).

The average static polarizability change upon electronic excitation ($\Delta\alpha$) was estimated from the following empirical formula (Table 2):[32]

$$\Delta\alpha = (-0.4 \pm 1.5) - [(18.2 \pm 1.4) \times 10^{-6}]pM, \qquad (3)$$

where molecular weight of the chromophore M is used as an effective cavity size parameter. The weight of the hydrocarbon portions of di-isopropylcarbinyl and dodecylthio substituents was excluded, since they can hardly screen the chromophore from the surrounding solvent.

Both the dispersive solvent shift and $\Delta\alpha$ increase appreciably upon *meso*-tetraaza substitution of the porphine ring (Figure 5). Further increase of both $|p|$ and $\Delta\alpha$ by a factor of 2 takes place in Pc's as a result of the annelation of benzo rings to tetraazaporphine structure. Solvent shifts of the Q bands in symmetric Pc's and Pc_3Nc's are quite similar. The unresolved S_1* + S_2* band of $Pc_3Nc(OCH_3)_2$* at 730 nm undergoes an identical shift with that of the S_1 band of the more stable form. Large scatter of data points in case of the second band in Pc_3-An shows that this band includes also the vibronic satellites of the S_1 transition. The hole-burning spectra also reveal a narrow vibronic hole in the broad background of the bleached S_2 transition.

The relationship between the solvent shifts and the strength of electron−phonon coupling will be discussed in the last section of this paper.

1.4. Absolute Orientation of Central Protons. The absorption of the product at 730 nm in both the room temperature spectra (Figure 4b) and in the photostationary state at 10 K (Figure 3b) is the strongest in the case of $Pc_3Nc(OCH_3)_2$. One can conclude that one of the protons in product state is attached to the naphthopyrrolic ring, because the predominantly electron-donating methoxy substituents enhance the negative charge density and, as a consequence, the proton affinity of the nearest pyrrolic nitrogen. Thus, the stable educt form should have both protons attached to the diagonal pair of identical benzopyrrolic rings. The Hammett parameter σ derived on basis of the acidity constants of substituted benzoic acids show that the electron-withdrawing capability increases in the order of *p*-OCH_3 (σ = −0.27) < H (0) = *p*-SCH_3 (0) < *m*-OCH_3 (0.12) < *m*-SCH_3 (0.15).[33] The naphthoic and anthracene carbonic acids are more acidic than the benzoic acid.[34] Therefore, the benzo substitution decreases the proton affinity of the carboxylate anion and probably the pyrrolic nitrogen in phthalocyanines, thus destabilizing the product state in Pc_3An. Indeed, the less stable tautomer has the lowest concentration in the photostationary state (Figure 3c) and is barely visible in the room-temperature spectra (Figure 4d) of Pc_3An. NMR spectra could be utilized in order to verify the conclusion about the proton attachment to the identical benzopyrrolic rings in the stable tautomer.

2. NH-Tautomerization Process. *2.1. NH-Tautomerizaion Equilibrium.* The relative amount of less stable tautomer trapped upon cooling of PEld samples in the dark is about 2% for Pc_3-Nc and 10% for $Pc_3Nc(OCH_3)_2$ (Figure 3a,b). At ambient temperature the equilibrium concentration of the product is higher, about 8% and 30% of the amount of educt, respectively (Figure 4a,b). The energy difference (ΔE) between the tautomers can be estimated according to the Boltzmann distribution law:

$$n_1/n_0 = \exp(-\Delta E/kT) \qquad (4)$$

where n_0 and n_1 are the populations of the lower and the upper levels, respectively. It follows from eq 4 that the ground state energy levels for the NH-tautomers of Pc_3Nc and its OCH_3 derivative differ by 520 and 250 cm^{-1}, respectively. Since the S_1 transition frequencies in the product are larger by 380 and 430 cm^{-1}, the energy separation in the fluorescent state is expected to be 900 and 680 cm^{-1} for Pc_3Nc and its OCH_3 derivative, respectively (see below, Figure 6). The relative stability of NH-tautomers of the isocycle containing porphine

TABLE 2: Solvent Shifts of Absorption Band Maxima of Tetrapyrrolic Pigments in *n*-Alkanes at 293 K[a]

compound	transition	ν_0 (cm^{-1})	$-p$ (cm^{-1})	r	N	$\nu(S_2)-\nu(S_1)$ (cm^{-1})	$\Delta\alpha$ (Å^3)[b]
Pe_3Nc	S_1	13 877 ± 6	2087 ± 24	8	0.9996	1110	23
	S_2	14 987 ± 15	2737 ± 64	8	0.9984		30
$Pc_3Nc(OCH_3)_2$	S_1	13 861 ± 14	2103 ± 57	8	0.9978		26
	S_1*	14 316 ± 4	2122 ± 17	6	0.99987		26
$Pc_3Nc(SC_{12}H_{25})_2$	S_1	13 892 ± 15	2393 ± 60	8	0.9981	975	25
	S_2	14 867 ± 16	2805 ± 66	7	0.9986		34
Pc_3An	S_1	13 490 ± 18	2231 ± 75	6	0.9977		26
	$S_2 + S_{11}$	14 107 ± 62	1210 ± 265	5	0.935		
	S_{21}	15 178 ± 77	3018 ± 320	6	0.978		36
t-Bu−TAP	S_1	16 326 ± 9	988 ± 39	7	0.9961	2323	9.3
	S_2	18 649 ± 22	1843 ± 92	7	0.9938		18
Pc[c]	S_1	15 022 ± 14 15 132[d,e]	2240 ± 59	6	0.9986		21
t-BuPc[f]	S_1	14 828 ± 34	1918 ± 138	7	0.987		25
	S_2	15 960 ± 60	2936 ± 249	7	0.982		38
porphine[c]	S_1	16 276 ± 6 16 320[d,g]	336 ± 24	6	0.976		1.5
chlorin[f]	S_1	15 857 ± 5 15 912[d]	659 ± 20	3	0.999		3.9

[a] ν_0, p, linear regression parameters of eq 1; r, correlation coefficient; N, number of solvents; $\nu(S_2)-\nu(S_1)$, extrapolated Q level splitting in free cold pigment molecule. [b] Average static polarizability change, eq 3. [c] Fluorescence band maxima. [d] 0−0 frequency in supersonic jet. [e] Reference 17. [f] Reference 30. [g] Reference 28.

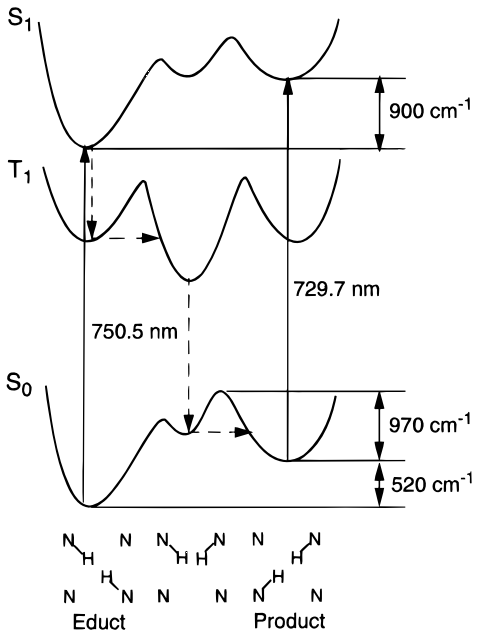

Figure 6. Potential energy diagram for the binding of protons in the center of a tetrapyrrolic pigment molecule. The nonradiative transition from the excited state of the educt to the ground state of the product is shown by dashed arrows. Energy differences between the tautomers in both the ground state and the first excited singlet state (520 and 900 cm^{-1}, respectively), the thermal activation energy of the product decay (970 cm^{-1}) and transition wavelengths of the tautomeric forms are indicated for Pc_3Nc in PEld.

derivatives is rather similar to our samples: 510 cm^{-1} in the ground and 150 cm^{-1} in the excited state.[18,24,25] By contrast to phthalocyanines and chlorins,[9,10] the product absorption of porphyrins is red shifted and, as a consequence, the energy difference in the excited state is less than that of the ground state.

2.2. Photoinduced Tautomerization. The hole-burning or the broad-band photobleaching quantum efficiency Φ was calculated as a ratio of the number of out-burned molecules to the amount of absorbed quanta. The bleached areas in the S_1 absorption bands were converted to the number of reacted molecules by using the following coefficients (number of molecules per cm^2 sample area, per (unit OD) (cm^{-1}), multiplied by 10^{13}): 1.39 (Pc_3Nc), 1.21 (Pc_3An), 5.2 (chlorin), and 69 (octaethylporphine).

TABLE 3: Phototautomerization (Hole-Burning) Quantum Yields at (Φ) 10 K

pigment	matrix[a]	Φ ($\times 10^{-3}$)	$\Phi/\Phi(D)$[b]	−/+10% of carotene[c]	$\Phi(80)/\Phi$[d]
Pc_3Nc	PEld	1.4 ± 0.3			
	PS	1.1 ± 0.2			
	PVB	1.1 ± 0.2	2.5	1.5	0.95, 1.1[e]
Pc_3Nc*[f]	PVB	8 ± 1	3	1.4	1.3, 1.3[e]
$Pc_3Nc(OCH_3)_2$	PS	0.8 ± 0.1			
$Pc_3Nc(SC_{12}H_{25})_2$	PS	0.8 ± 0.1			
Pc_3An	PEld	1.5 ± 0.2			
	PS	2.2 ± 0.5			
Pc_3An*[f]	PEld	9 ± 2			
OEP	PMMA	25 ± 5	21	1.7[g]	
chlorin	PS	0.3 ± 0.05		2.8	
chlorin*[f]	PS	100 ± 20			

[a] PEld, low-density polyethylene; PS, polystyrene; PVB, poly(vinyl butyral); PMMA, poly(methyl methacrylate). [b] Deuterium isotope effect. [c] Change of Φ in the matrix containing 10% of β-carotene. [d] Ratio of Φ at 80 and 10 K. [e] For deuterated compound. [f] Less stable tautomer. [g] In PVB.

The hole formation quantum yields for protonated and deuterated pigments are summarized in Table 3. The quantum yield of photoconversion for the stable tautomer lies between 10^{-3} and 2×10^{-3} for mixed (na)phthalocyanines and is practically independent on the host polymer and temperature (up to 80 K). The exchange of protons to deuterons was carried out by keeping the doped PVB films in D_2O vapours at room temperature for 2−3 days. The hole-burning rate is slowed down in deuterated samples by a factor of 2.3 (Pc_3Nc), 3 (Pc_3Nc*), or even 21 (OEP). Considerable retardation of the hole burning (by factor of 18−45) in water-soluble porphyrins has been reported recently.[35]

The role of triplet state was explored in the samples containing 10% (w/w) of β-carotene. At such a high concentration the β-carotene is expected to quench the triplet state of pigments by means of an exchange-type energy transfer. A decrease of the burning rate by a factor of 1.5−2.8 was observed. Consequently, the energy transfer to β-carotene confirms the involvement of the triplet state, established earlier for protopheophytin by using the heavy-atom quenching.[25]

Possible mechanism of the prototropic phototransformation is still under discussion in the literature.[25,36−38] It has been found that in the presence of ethyl iodide both the phosphorescence and the phototautomerization of nonsymmetrically substituted

porphyrins can be quenched by a factor of 5−10.[25] It has been concluded that the energetically strongly allowed proton shift in the course of nonradiative processes should be of minor importance, despite the large probabilities of nonradiative $S_1 \rightarrow T_1$ and $T_1 \rightarrow S_0$ decays (>0.5) and the large amount of dissipated energy ($(1-2) \times 10^4$ cm^{-1}). It is likely also in our case that the reaction takes place on the T_1 potential surface rather than during the vibrational relaxation. Between 10 and 80 K the temperature has a negligible effect on Φ, regardless on the direction of the process (Table 3). Since no thermal activation of the photoreaction is needed, the T_1 potential surface must have a minimum with adjacent protons, serving as an intermediate state of the photoinduced NH-tautomerization. The alternative synchronous shift of two protons to the diagonal N atoms can be ruled out, because in this case only a half of the inhomogeneous ensemble of symmetrical porphyrin molecules would be phototransformable at very low temperatures. Indeed, for statistical reasons, nearly isoenergetic states with the turned proton pairs should have higher energy in 50% of cases. Such a retardation of hole burning is not observed in D_{2h} porphyrins.

Thus, one should admit that the configuration with adjacent protons can be the most stable in the triplet state. Note that there are two such a states in Chl and $NcPc_3$. Therefore, the rate-limiting and isotope-sensitive step should be the tunneling of one of the protons, which results in the *cis*-structure. The structure with adjacent protons is formed in the triplet state with low yield in the order of magnitude of Φ. If the population of this triplet-state global minimum would be rapid, the hole-burning quantum yield would probably reach 0.5 in symmetrical porphyrins.

The hole-burning efficiency shows a pronounced dependence on axial inequivalence of the molecule. The Φ value in OEP is as high as 2.5%, whereas in chlorin it is 0.03% (Table 3). The stable form of slightly asymmetric (na)phthalocyanines burns with a yield about 0.1%. Less stable tautomers show a reversed behavior. In particular, Chl* can be converted back to the educt with a high yield Φ = 10%. For Pc_3An* and Pc_3-Nc*, the corresponding Φ value is by a factor of 6−8 larger that of the educt state (in protonated species). For Chl/Chl* the Φ ratio reaches 300. Both the influence of asymmetry of the molecule and various reactivity of tautomers can be explained with the aid of Figure 6. The decay route (partition ratio) of the unstable molecule with adjacent protons in the ground state (in the middle) obviously depends on the barriers in the two reaction paths leading to the configurations with diagonal protons. Because, in general, the deeper minima can be reached faster, the product formation process slows down and its decay becomes faster if the asymmetry of the molecule increases.

2.3. Thermal Decay of the Product. In order to study the thermal stability of the product, first a considerable amount of less stable tautomer was accumulated under the irradiation of Pc_3Nc derivatives in PEld and PVB films with white light at 10 K. Then the temperature was gradually rised and the absorption spectra were recorded in every 15 min. The decay of less stable tautomer sets in at about 70 K and at 140 K practically all the photoaccumulated product has disappeared (Figure 7). The normalized change of optical density or the integrated area of the product or educt absorption bands was plotted as a function of temperature (Figure 8). In Chl and Pc_3-Nc, half of the product absorption disappears at 51 and 115 K, respectively. For deuterated pigments this temperature is somewhat higher, 61 and 153 K. Analogous isotopic effect has been obtained for porphine doped in *n*-hexane crystals.[39] The product decay and the educt accumulation curves can be approximated with integrated Gaussians. The latter may be regarded as distribution functions of reaction barriers (Figure 9).

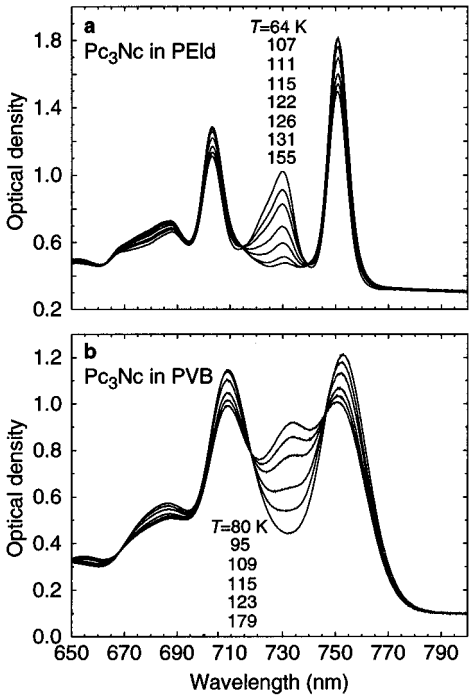

Figure 7. Temperature dependence of the absorption spectra of the photostationary mixture of NH-tautomers, produced during the exposure with white light (100 s, 100 mW/cm^2) at 10 K. The absorption decay of the product at 730 nm is observed as the temperature increases from the top to the bottom of the column as indicated.

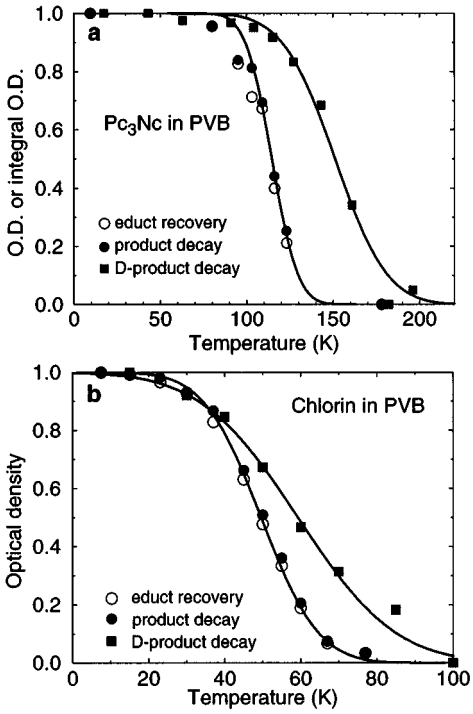

Figure 8. Normalized temperature-induced decay of the phototautomer and the recovery of educt for Pc_3Nc (a) and chlorin (b) in PVB monitored at their respective absorption maxima. Lines are the fittings with the integrated Gaussian functions (see Figure 9).

Low half-recovery temperature (T_m = 51 K) in chlorin shows that the other tautomeric form is very unstable (Table 4). Similar values have been reported for Chl* in glassy (T_m = 50 K) or crystalline benzophenone host (T_m = 30−45 K).[40] The Pc_3Nc* (T_m = 115−117 K) is slightly less stable than the broad

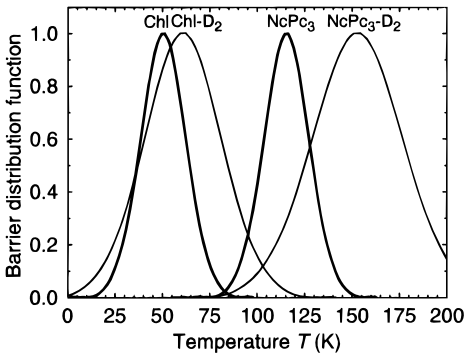

Figure 9. Gaussian distributions of reaction barriers for the photoproduct decay in chlorin and Pc_3Nc in PVB matrix. The widths and maxima of the distribution functions are given in Table 4.

TABLE 4: Thermal Decay of the Photoaccumulated Product: The Half-Decay Temperature (T_m) and FWHM (ΔT) of the Gaussian Barrier Distribution Function[a]

pigment	matrix[b]	T_m (K)	ΔT (K)
Pc_3Nc	PEld	117	27
	PVB	115	30
Pc_3Nc-D_2	PVB	153	56
chlorin	PVB	51	28
chlorin$-D_2$	PVB	61	47

[a] FWHM, full-width at half-maximum. [b] PEld, low-density polyethylene; PVB, poly(vinyl butyral).

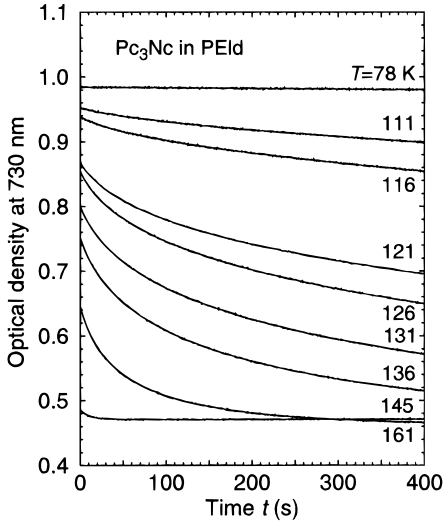

Figure 10. Temperature dependence of the decay kinetics of photoaccumulated tautomer Pc_3Nc^* in low-density polyethylene measured at 730 nm in time drive mode of Perkin Elmer Lambda 9 spectrophotometer. The photostationary state was created at the same temperature (indicated on the right-hand side) by irradiating with white light (100 s, 100 mW/cm^2) before the recording was started.

holes burned in the parent phthalocyanine and its substituted derivatives in PMMA matrix (T_m = 124−126 K).[41] The deuterated Pc_3Nc^* is as stable thermally as the spectral holes burned in the S_1 band of *meso*-tetrapropylporphine in PMMA matrix (T_m = 152 K).[41]

The decay kinetics at constant T can be followed also in the time scale. Figure 10 shows the decay curves of photostationary state in the dark at different T. The sample was first exposed to the white light (100 mW/cm^2) during 100 s at fixed T. Then the recording set at the Pc_3Nc^* maximum (730 nm) was started as fast as possible (in 1−2 s) in the time drive mode of the spectrophotometer. No decay is observed below 80 K. This fact proves also that depleaching caused by the monitoring light of the apparatus is negligible. At higher T the kinetics becomes

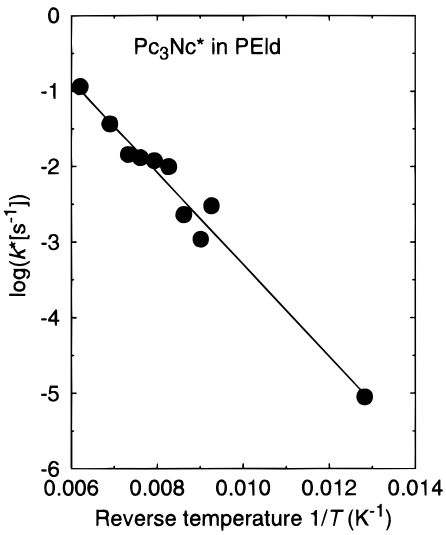

Figure 11. Arrhenius plot for the temperature dependence of the effective first-order decay constant of the photoaccumulated tautomer Pc_3Nc^* in low-density polyethylene (see Figure 10). The slope of the line corresponds to the activation energy of 970 cm^{-1} (eq 6).

faster. Also, the initial optical density of the product in the photostationary state decreases. Finally, above 160 K the initial amount of Pc_3Nc^* becomes so small and its decay so fast that the kinetics cannot be followed any more in this experiment.

The kinetic curves were fitted with a stretched exponential function[41] in the following form:

$$\ln(\mathrm{OD} - \mathrm{OD}_0) = a_0 - k^*(t)^{a_2} \qquad (5)$$

Parameter a_2 changes in a rather narrow interval between 0.55 and 0.65. We treat k^* as an effective first order rate constant of a monomolecular process. In this case the Arrhenius activation energy E_A can be obtained as a slope of the plot of log k^* vs $1/T$ (Figure 11):

$$\log k^* = (2.79 \pm 0.31) - (609 \pm 36)/T,\ N = 10,\ r = 0.986, \qquad (6)$$

$$E_A = (2.303)(609)(0.69) = 970\ \mathrm{cm}^{-1}$$

where N is number of data points and r is the correlation coefficient.

The thermal decay of the photoaccumulated less stable tautomer ought to be characterized as a thermally activated tunneling process because it is sensitive to deuteration.

3. Electron-Phonon Coupling. *3.1. Debye−Waller Factors.* The Debye−Waller factor (DWF), or the relative probability of zero-phonon transition, is one of the key parameters of hole-burning materials. The zero-phonon transition intensity increases with the lowering of temperature as the number of phonons is diminished. There is always a finite probability of creating phonons that gives rise to the anti-Stokes part of the phonon wing even at T = 0 K. The DWF was determined as $z^{1/2}$, where z is the ratio of zero-phonon hole area to the total loss of absorption intensity. The DWFs of Pc_3Nc's, Chl, and OEP at 8 K are listed in Table 5. Because the magnitude of kT at 8 K is less than the peak maximum of the phonon wing (10−18 cm^{-1}) (see below), the measured DWFs are close to the maximum values at low-temperature limit.

For pigments doped in the same host matrix, PS, the DWF decreases in the order of OEP (0.87) > Chl (0.70) > Pc_3Nc (0.62). A slight diminishing of DWF occurs in the series of (na)phthalocyanines: $Pc_3Nc(OCH_3)_2$ > Pc_3Nc > Pc_3Nc-

TABLE 5: Debye−Waller Factors (DWF), Phonon Wing Maxima (ν_{ph}),[a] and Temperature Dependence of Quasihomogeneous Hole Width (Γ_{qh}) in Pigment/Polymer Systems

						$\Gamma_{qh} = a_0 + a_1 T^{a_2}$ [e]			
pigment	polymer[a]	DWF[b]	ν_{ph} (cm^{-1})[c]	Γ_{qh} (15 K) (GHz)[d]	Γ_{qh} (25 K) (GHz)[d]	a_0(GHz)	a_1	a_2	ΔT (K)[f]
Pc_3Nc	PEhd		17.5	1.5	12	−2.3	0.0035	2.59	8−44
	PEld	0.71	17.5	1.5	14.5	−2.6	0.0057	2.49	10−45
	acrPhP		16	59	117	−9	2.71	1.19	4−26
	olPhP		14.4	19	54	0.3	0.048	2.19	6−40
	PS	0.62	10.2	48	142	9.6	0.057	2.40	8−26
	PVB	0.70	16.8	9.4	39	−0.8	0.0069	2.69	6−40
Pc_3Nc*[g]	PEld	(0.46)	17.5	4.5	20	1.8	0.00051	3.22	10−45
$Pc_3Nc(OCH_3)_2$	PS	0.63		52	∼140	−2.5	0.35	1.86	7−24
$Pc_3Nc(SC_{12}H_{25})_2$	PS	0.60		58	137	11.3	0.191	2.02	6−25
Pc_3An	PS			73					
	PVB	0.63							
	PEld	0.75							
Pc_3An*[g]	PEld	0.73							
octaethylporphine	PEld				8	−3.2	0.00186	2.68	17−50
	PS	0.87	∼10	25	68	−0.6	0.139	1.93	8−33
chlorin	PS	0.70	∼10	42	109	−4.6	0.47	1.71	8−23
chlorin*[g]	PS	<0.15							

[a] PEhd, high-density polyethylene; PEld, low-density polyethylene, acrPhP, acrylic photopolymer; olPhP, olefinic photopolymer; PS, polystyrene; PVB, poly(vinyl butyral). [b] At 8 K; relative error ±5%. [c] Error ±1 cm^{-1}. [d] Quasihomogeneous hole width at 15 and 25 K, relative error ±10%. [e] a_0−a_2 are the fitting parameters. [f] Temperature interval of the fitting. [g] Less stable tautomer.

$(SC_{12}H_{25})_2$. Similar DWFs are obtained for Pc_3An and its less stable tautomer Pc_3An*. The effective DWF for the product state of Pc_3Nc (0.46) is smaller than that of the educt (0.62). However, that does not mean that linear electron−phonon coupling (EPC) of the S_1 transition is stronger in the product state. Since in Pc_3Nc* the S_1 band overlaps strongly with the S_2 band, the bleaching of the latter contributes to the broad background of the narrow zero-phonon hole, leading to the apparent decrease of measured DWF. As far as the influence of the host matrix is concerned, DWF and, therefore, the achievable hole-to-background contrast is much higher in PE and PVB as compared to PS. For a recent study of EPC in many polymer hosts, see ref 42.

The dependence of DWF on host properties and the nature of electronic transition in the pigment molecule can most conveniently be discussed in terms of Franck−Condon principle for low-frequency intermolecular vibrations. Large change in intermolecular forces upon electronic excitation results in the high probability of phonon creation in the course of an optical transition, and vice versa.[8] In molecular solids, the dispersive and (induced) dipole−dipole interactions prevail. As a consequence, the change of polarizability and dipole moment upon electronic excitation of the pigment molecule on one hand, and the presence of dipolar or quadrupolar groups in the surrounding matrix on the other hand, determine the strength of EPC in impurity molecules. Therefore, the solvent shifts and intermolecular vibronic coupling processes are closely related.[8]

Accordingly, the S_1 transitions with the highest values of DWF in prophine and its alkyl-substituted derivatives undergo negligible solvent shifts. The reduction of the pyrrole ring in chlorins and the *meso*-tetraaza substitution increase both the strength of linear EPC and the slope of dispersive solvent shift equation $|p|$ (eq 2) (Table 2). According to the Bakhshiev theory[32,43] (eqs 2 and 3), the dispersive solvent shift is proportional to the polarizability density difference between the ground and the excited state ($\Delta\alpha/r^3$, r is the Onsager cavity radius). The change of intermolecular London and induced-dipole−permanent-dipole forces on electronic excitation depends critically on the same parameter. The change in intermolecular potentials couples the electronic transition to soft intermolecular modes ("phonons").

Indeed, a clear-cut dependence between the DWFs in PS for OEP (0.87), Chl (0.70), and Pc_3Nc (0.62) and dispersive solvent shifts per unity Lorentz−Lorenz function (p) holds, with $|p|$ = 128, 659,[30] and 2087 cm^{-1} (Table 2), respectively.

3.2. Quasihomogeneous Hole Width. The width of persistent holes which are burned and recorded at the same temperature will be discussed below. The hole widths obtained from this experiment are denoted as quasihomogeneous (Γ_{qh}), since during the measurement the spectral diffusion occurring in time scales longer than excited-state lifetime may contribute to the hole width. The dephasing times calculated in accordance with uncertainty relation as one-half of the permanent hole width tend to be shorter than those measured directly by phonon echo methods.[44]

The temperature dependence of Γ_{qh} is shown in Figure 12a−c. In case of Pc_3Nc, the hole width at a fixed temperature (e.g., 15 or 25 K) can vary by more than an order of magnitude in different matrices (Table 5). The width increases in the following order of hosts: PEhd ≤ PEld < PVB < olefinic photopolymer < acrylic photopolymer ∼ PS. Only a very slight broadening is observed within a series of different mixed (na)-phthalocyanines in PS matrix: $Pc_3Nc \sim Pc_3Nc(OCH_3)_2 \leq Pc_3Nc(SC_{12}H_{25})_2 < Pc_3An$. A comparison with octaethylporphine and chlorin in PS and PEld reveals the phthalocyanines are subject to a stronger broadening. A correlation with dispersive solvent shifts and the polarizability differences between the ground and the excited state is obvious also for quadratic EPC strength, similarly to the linear EPC.[8]

Concerning the influence of environment on optical dephasing rates, two parameters are of main importance: the phonon density of states and the matrix polarity.[42] The phonon spectrum of the host matrix closely resembles the pseudowing contour in a strongly burned spectrum.[42] The absorption difference spectra before and after the burning (hole-burning spectra) are shown in Figure 13. The irradiation with a large dose leads to the phototransformation of most of the molecules having the 0-0 line in resonance with the laser frequency. In addition, a large number of molecules excited via the phonon wing absorption which has much smaller cross section is bleached. This gives rise to a broad pseudo wing on the long-wavelength side of the hole. The absorption maximum of the pseudowing (ν_{ph}) gives approximately the frequency of low-energy modes which are most strongly coupled to the electronic transition. In the T range under investigation the thermal energy kT is in the order magnitude of the phonon sideband maximum ν_{ph}. The

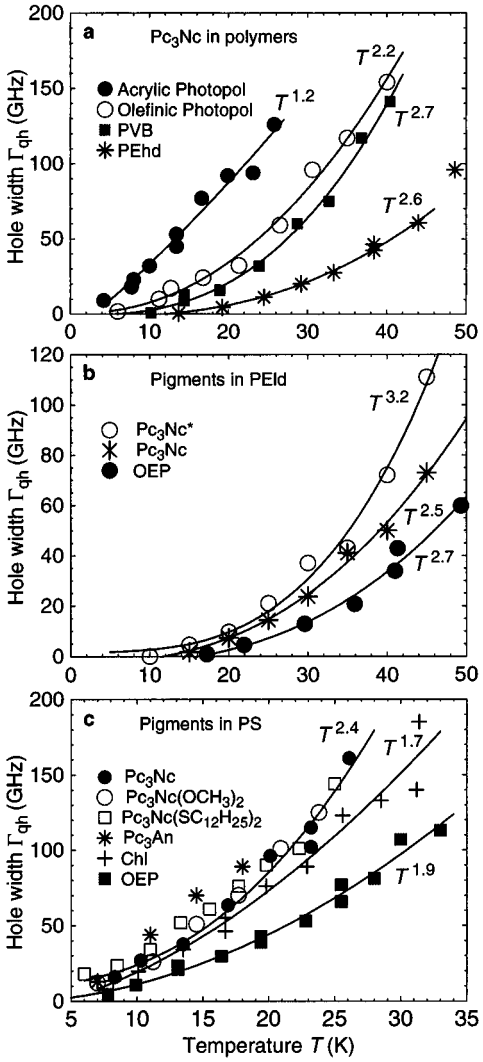

Figure 12. Temperature dependence of quasihomogeneous hole width in different polymer hosts doped with Pc_3Nc (a) as well as in polyethylene (b) and polystyrene (c) doped with different phthalonaphthalo/anthracenocyanines, chlorin, and octaethylporphine. Lines represent the power-law fittings of experimental data, the temperature coefficient of which is indicated. Only the fitting curve for Pc_3Nc is shown in (c). The hole widths at 15 and 25 K and the parameters of the fitting lines are listed in Table 5.

vibrational modes contributing to the wing contours are thermally excited and can lead to the electronic dephasing and line broadening in impurity molecules.

The holes in nonpolar polyolefin matrices are much narrower than those in polar environments. Particularly small Γ_{qh} values are obtained in PE which has relatively high phonon sideband frequency ($\nu_{ph} = 17.5$ cm^{-1}). Spectral bandwidths in saturated hydrocarbons, including PE, are narrow since the electric moments are very small in these systems. PVB belongs also to the matrices with narrow impurity lines, because of the presence of aliphatic hydrocarbon fragments ($-C_3H_7$) and, plausibly, certain cross-linking effect by the residual hydrogen bonds ensuring a fairly large value of ν_{ph} (17 cm^{-1}). The strongest EPC in PS is associated with the low phonon frequency (10 cm^{-1}) and large quadrupole moments of the aromatic sidegroups in this polymer. The presence of fluctuating electric fields in the matrix can modulate the transition frequency of impurity molecules by means of the linear and quadratic Stark effect and thus provide an efficient hole broadening mechanism. Despite the quite large value of phonon frequency ($\nu_{ph} = 16$ cm^{-1}), the acrylic photopolymer is an unfavorable host, obviously, as a result of polarity. The olefinic photopolymer is less polar and nearly as suitable for embedding photochromic dye molecules as PVB.

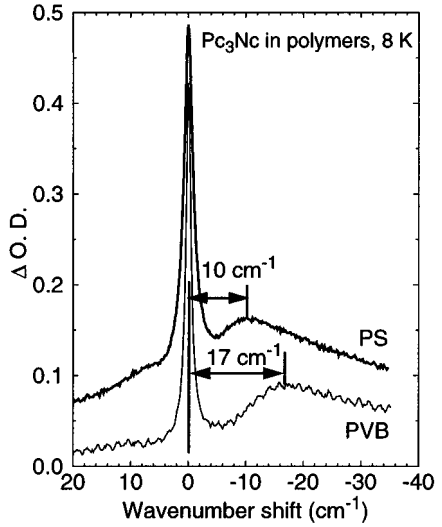

Figure 13. Inverted absorption change in the spectra of Pc_3Nc in polystyrene and poly(vinyl butyral) upon hole burning with a large light dose of 40 mJ/cm^2 at 756.5 nm (PS) or 20 mJ/cm^2 at 752 nm (PVB). The maximum position of the pseudo phonon sideband with respect to the resonant hole at the zeroth wavenumber is indicated. The curve for PS is upshifted by 0.05 O.D. units.

Conclusions

Unsymmetrically substituted phthalonaphthalocyanines were specially designed and synthesized with the aim to meet the requirements to the photochroms suitable for spectral hole-burning applications. In particular, the spectral separation of the educt and product, the strong 0-0 absorption in resonance with the Ti:sapphire laser (750−780 nm) and excellent solubility in polymers were achieved. The most relevant properties of these novel hole-burning materials, such as the quantum yields, Debye−Waller factors, and quasihomogeneous hole widths, were measured and compared with the respective parameters for chlorins and porphyrins. With the hole-burning efficiency of about 10^{-3}, the phthalocyanines occupy an intermediate position between simple porphyrins ($\Phi \sim 10^{-2}$) and chlorins ($\Phi \sim 10^{-4}$).

Common features in the spectral properties of tautomeric forms of three groups of asymmetrical tetrapyrrolic macrocycles (phthalocyanines, chlorins, and porphyrins) were pointed out. It was established that the average energy of Q transitions remains nearly constant for both tautomers. The S_1 band of the less stable form is blue shifted in Pc's and chlorins and red shifted in porphyrins. The distance between the S_1 bands of tautomers is approximately equal to S_1-S_2 splitting in the Zn (Mg) complex of the same ligand. The larger is the spectral separation between the NH-tautomers, the less efficient is the hole burning in the stable form and vice versa. The photoinduced migration of protons probably occurs via the stable *cis* configuration on the triplet potential surface.[25]

For different dyes, a relationship between the dispersive solvent shifts of transition energies and the strength of electron−phonon coupling was established and explained. The tetraaza and benzo substitution in phthalocyanines increases the polarizability of the excited state and, as a result, increases the strength of EPC. With a proper selection of the matrix it is still possible to achieve the DWF as high as 0.75. The weakest coupling is observed in nonpolar polyolefin hosts with high

characteristic phonon frequencies. In polar polymers, the DWFs are smaller and the holes are considerably broader.

Acknowledgment. We thank N. Bogdanova-Arn and A. Mühlebach (Ciba) for preparation of photopolymers doped with pigments and G. Grassi (ETH) for synthesis of chlorin. We are grateful to O. Ollikainen (Institute of Physics, Tartu, Estonia) for suggesting the use of the two-channel detection of holes with the Molectron Joulemeter and W. Ferri (ETH) for supplying a data transfer program for this purpose. This work was supported by the KWF Grant 2296.1 and ETH Zürich.

References and Notes

(1) Gorokhovskii, A. A.; Kaarli, R. K.; Rebane, L. A. [*Zh. Eksp. Teor. Fiz., Pis'ma Red.* **1974**, *20*, 474] [*JETP Lett.* **1974**, *20*, 216].

(2) Kharlamov, B. M.; Personov, R. I.; Bykovskaya, L. A. *Opt. Commun.* **1974**, *12*, 191.

(3) Renge, I. Unpublished data.

(4) Rebane, A.; Kaarli, R. *Chem. Phys. Lett.* **1983**, *101*, 317. Rebane, K. K.; Rebane, A. K. In *Molecular Electronics*; Mahler, G., May, M., Schreiber, M., Eds.; Marcel Dekker: New York, 1996; Chapter, 13, pp 257−302.

(5) Renn, A.; Meixner, A. J.; Wild, U. P.; Burkhalter, F. A. *Chem. Phys.* **1985**, *93*, 157.

(6) De Caro, C.; Bernet, S.; Renn, A.; Wild, U. P. In *Molecular Electronics*; Mahler, G., May, M., Schreiber, M., Eds.; Marcel Dekker: New York, 1996; Chapter 14, pp 303−332.

(7) Maniloff, E. S.; Altner, S. B.; Bernet, S.; Graf, F. R.; Renn, A.; Wild, U. P. *Appl. Opt.* **1995**, *34*, 4140. Plagemann, B. H.; Gnal, F. R.; Altner, S. B.; Renn, A.; Wild, U. P. *Appl. Phys. B.* **1997**, in press.

(8) Renge, I. *J. Opt. Soc. Am. B* **1992**, *9*, 719.

(9) Völker, S.; Macfarlane, R. M. *J. Chem. Phys.* **1980**, *73*, 4476.

(10) Dicker, A. I. M.; Noort, M.; Thijssen, H. P. H.; Völker, S.; van der Waals, J. H. *Chem. Phys. Lett.* **1981**, *78*, 212.

(11) Rebane, A.; Ollikainen, O.; Schwoerer, H.; Erni, D.; Wild, U. P. *J. Lumin.* **1995**, *64*, 283.

(12) Bhattacharjee, D.; Popp, F. D. *J. Heterocycl. Chem.* **1980**, *17*, 315.

(13) Japanese Patent 2178545, *Sumitomo Chem. Ind.*

(14) Hallman, J. L.; Bartsch, R. A. *J. Org. Chem.* **1991**, *56*, 6243.

(15) Kitahara, K.; Asano, T.; Hamano, K.; Tokita, S.; Nishi, H. *J. Heterocycl. Chem.* **1990**, *27*, 2219.

(16) Gouterman, M. In *The Porphyrins*; Dolphin, D., Ed.; Academic Press: New York, 1978; Vol. III, Chapter 1, pp 1−165.

(17) Fitch, P. S. H.; Haynam, C. A.; Levy, D. H. *J. Chem. Phys.* **1980**, *73*, 1064.

(18) Gurinovich, G. P.; Zenkevich, E. I.; Shulga, A. M. In *Porphyrins. Excited States and Dynamics*; Gouterman, M., Rentzepis, P. M., Straub, K. D., Eds.; ACS Symposium Series 321; American Chemical Society: Washington, DC, 1986; Chapter 5, pp 74−93.

(19) Avarmaa, R. A.; Suisalu, A. P. *Opt. Spektrosk.* **1984**, *56*, 53 [*Opt. Spectrosc.* **1984**, *56*, 32].

(20) Arabei, S. M.; Egorova, G. D.; Solov'ev, K. N.; Shkirman, S. F. *Zh. Prikl. Spektrosk.* **1986**, *44*, 117 [*J. Appl. Spectrosc.* **1986**, *44*, 96].

(21) Keegan, J. D.; Stolzenberg, A. M.; Lu, Y.-C.; Linder, R. E.; Barth, G.; Moscowitz, A.; Bunnenberg, E.; Djerassi, C. *J. Am. Chem. Soc.* **1982**, *104*, 4317.

(22) Gradyushko, A. T.; Solov'ev, K. N.; Tsvirko, M. P. *Opt. Spektrosk.* **1978**, *44*, 1123 [*Opt. Spectrosc.* **1978**, *44*, 656].

(23) Mauring, K.; Avarmaa, R. *Chem. Phys. Lett.* **1981**, *81*, 446.

(24) Zenkevich, E. I.; Shulga, A. M.; Filatov, I. V.; Chernook, A. V.; Gurinovich, G. P. *Chem. Phys. Lett.* **1985**, *120*, 63.

(25) Dvornikov, S. S.; Kuzmitskii, V. A.; Knyukshto, V. N.; Solov'ev, K. N. *Dokl. Akad. Nauk. SSSR* **1985**, *282*, 362. Dvornikov, S. S.; Kuzmitskii, V. A.; Knyukshto, V. N.; Solov'ev, K. N.; Turkova, A. E.; Ivanov, E. G. *Khim. Fiz.* **1985**, *4*, 889 [*Sov. J. Chem. Phys.* **1987**, *4*, 1455].

(26) Michl, J.; Thulstrup, E. W. *Spectroscopy with Polarized Light*; VCH Publishers: New York, 1986.

(27) *Landolt-Börnstein, Zahlenwerte und Funktionen* II/8; Springer: Berlin, 1962. *Aldrich Catalog Handbook of Fine Chemicals 1994−1995*; Aldrich Chemical Company, Inc.: Milwaukee, WI, 1994.

(28) Even, U.; Jortner, J. *J. Chem. Phys.* **1982**, *77*, 4391.

(29) Renge, I. *J. Photochem. Photobiol., A* **1992**, *69*, 135.

(30) Renge, I. *J. Phys. Chem.* **1993**, *97*, 6582.

(31) Renge, I. *J. Phys. Chem.* **1995**, *99*, 15955.

(32) Renge, I. *Chem. Phys.* **1992**, *167*, 173.

(33) Hansch, C.; Leo, A. *Substituent Constants for Correlation Analysis in Chemistry and Biology*; J. Wiley: New York, 1979.

(34) Kortüm, G.; Vogel, W.; Andrussow, K. *Dissoziationskonstanten organischer Säuren in Wässriger Lösung*; Butterworths: London, 1961. Serjeant, E. P.; Dempsey, B. *Ionization Constants of Organic Acids in Aqueous Solution*; IUPAC Chemical Data Series No. 23; Pergamon: Oxford, 1979.

(35) Sakoda, K.; Maeda, M. *Chem. Phys. Lett.* **1994**, *217*, 152.

(36) Borisevich, E. A.; Knyukshto, V. N.; Kozyrev, A. N.; Solovyev, K. N. *Opt. Spektrosk.* **1993**, *74*, 210 [*Opt. Spectrosc.* **1993**, *74*, 129].

(37) Zenkevich, E. I.; Shulga, A. M.; Chernook, A. V.; Gurinovich, G. P. *Khim. Fiz.* **1987**, *6*, 1212 [*Sov. J. Chem. Phys.* **1990**, *6*, 2384].

(38) Radziszewski, J. G.; Waluk, J.; Nepras, M.; Michl, J. *J. Phys. Chem.* **1991**, *95*, 1963.

(39) Butenhoff, T. J.; Moore, C. B. *J. Am. Chem. Soc.* **1988**, *110*, 8336.

(40) Schellenberg, P.; Friedrich, J.; Kikas, J. *J. Chem. Phys.* **1994**, *101*, 9262.

(41) Kümmerl, L.; Kliesch, H.; Wöhrle, D.; Haarer, D. *Chem. Phys. Lett.* **1994**, *227*, 337. Kümmerl, L. G. PhD Thesis, University of Bayreuth, Germany, 1994.

(42) Renge, I. *J. Chem. Phys.* **1997**, *106*, 5835.

(43) Bakshiev, N. G.; Girin, O. P.; Piterskaya, I. V. *Opt. Spektrosk.* **1968**, *24*, 901 [*Opt. Spectrosc.* **1968**, *24*, 483].

(44) Zimdars, D.; Fayer, M. D. *J. Chem. Phys.* **1996**, *104*, 3865.